Annals of Microbiology (2019) 69:457–468
https://doi.org/10.1007/s13213-018-1431-2

ORIGINAL ARTICLE

Transcriptomic and metabolomics analyses reveal metabolic characteristics of L-leucine- and L-valine-producing *Corynebacterium glutamicum* mutants

Yuechao Ma[1,2,3] · Qian Ma[1,2,3] · Yi Cui[1,2,3] · Lihong Du[1,2,3] · Xixian Xie[1,2,3] · Ning Chen[1,2,3]

Received: 14 June 2018 / Accepted: 28 December 2018 / Published online: 10 January 2019

Abstract

Industrial amino acid production strains of *Corynebacterium glutamicum* are usually obtained by mutagenesis. However, the genetic and metabolic characteristics and the efficient synthesis mechanism of the selected mutants are unclear. The aims of this study were (1) to determine the gene transcriptional patterns and intracellular metabolite levels of an L-leucine-producing mutant *C. glutamicum* CP and an L-valine-producing mutant *C. glutamicum* XV referring to wild type, and (2) to understand the efficient synthesis mechanism of target product of these mutants. For this purpose, transcriptomic and metabolomics analyses were combined to investigate the association between intracellular patterns and product synthesis. The high intracellular level of glucose and the low intracellular level of metabolites in the central carbon metabolism meant the glucose metabolism rate of two mutants was lower than wild type. However, the increased intracellular pentose level and gene transcription in the pentose phosphate pathway (PPP) indicated that the PPP of mutants was more active. Furthermore, the mutants showed higher intracellular level of NADPH, which was mainly generated in PPP. In the specific pathway for the synthesis of L-leucine and L-valine, the transcriptional level of most genes was upregulated in the mutants. However, the transcription of transaminase C coding gene *Cgl2844* was downregulated in CP but upregulated in XV. The upregulation of *Cgl2844* might benefit to the synthesis of L-valine and cause the significant decrease of intracellular level of L-alanine and L-glutamate of XV. These characteristics of the mutants provided insight into changes that could be made to systematically optimize the metabolic pathways for the production of L-leucine and L-valine.

Keywords *Corynebacterium glutamicum* · Transcriptomic · Metabolomics · L-valine · L-leucine

Yuechao Ma and Qian Ma contributed equally to this work and should be considered as co-first authors

Electronic supplementary material The online version of this article (https://doi.org/10.1007/s13213-018-1431-2) contains supplementary material, which is available to authorized users.

✉ Xixian Xie
xixianxie@tust.edu.cn

✉ Ning Chen
ningch@tust.edu.cn

[1] National and Local United Engineering Lab of Metabolic Control Fermentation Technology, Tianjin University of Science & Technology, Tianjin 300457, People's Republic of China

[2] Key Laboratory of Microbial Engineering of China Light Industry, Tianjin University of Science & Technology, Tianjin 300457, People's Republic of China

[3] College of Biotechnology, Tianjin University of Science & Technology, Tianjin 300457, People's Republic of China

Introduction

Corynebacterium glutamicum is a Gram-positive bacterium with high G+C content that is able to utilize a variety of sugars and organic acids as a carbon source. It has been engineered as a workhorse for the industrial production of various amino acids and other chemicals, materials, and fuels of interest (Okino et al. 2005). The high production of branched-chain amino acids (BCAA) is an important potential application of *C. glutamicum* (Vogt et al. 2014). However, the extensive synthesis pathway and strict feedback regulation of BCAA synthesis make the construction of engineering BCAA-producing strain difficult. Strains used in industrial BCAA production are ideal materials to investigate the genetic advantages that facilitate BCAA synthesis. However, the genetic characteristics of these industrial strains, including gene transcription patterns and intracellular metabolite levels, are

rarely reported. Additionally, since these strains have traditionally obtained by classical random mutagenesis and selection approaches, the genomic identity of these mutants is often unclear (Leuchtenberger 1996). This obscures the efficient synthesis mechanism of the BCAA-producing strains and restricts their further development and improvement. There are many advantages to the introduction of mutants to utilize a metabolic engineering BCAA-producing strain with a defined genetic background, and this is a low-cost and efficient strategy (Becker et al. 2011). However, this requires understanding the mutations present in the strain and how these mutants are altering BCAA synthesis. To address this, a comprehensive analysis of the biological system of those mutants is required using omics (Yang and Yang 2017).

Transcriptomic analysis has become a key research tool for metabolic engineering. Genome-wide transcriptomic analysis can help us better understand the transcriptional regulation mechanisms of *C. glutamicum* (Muffler et al. 2002; Solieri et al. 2013). This approach has been used to enhance tolerance to extreme environment, improve cell growth, and increase target product synthesis in *C. glutamicum* (Chen et al. 2016; Inui et al. 2007). Besides, by employing proteomics method, the expression abundance of proteins can be analyzed. A previous report investigated the changes of both gene transcription and protein expression between a *C. glutamicum* mutant and parent strain to understand the mechanism of high L-valine production (Zhang et al. 2018). In addition, a comprehensive metabolomics analysis can be used at the same time to reveal any changes in the amounts of the compounds affecting relevant metabolic pathways for BCAA synthesis, such as gene products involved in central carbon metabolism and amino acid metabolism (Bartek et al. 2008). Overall, a combination of transcriptomic, proteomics, and metabolomics analyses contributes to cognize cell metabolic characteristics based on changes in both gene transcription, protein expression, and intracellular metabolite levels (Krömer et al. 2004). This approach could help to systematically optimize the metabolic pathways for improved BCAA production in *C. glutamicum*.

The L-leucine-producing strain *C. glutamicum* CP and the L-valine-producing strain *C. glutamicum* XV were obtained after traditional repeated processes of random mutation and selection. In our previous work, a comparative genomic analysis was performed to identify the genomic variations between these two mutants and wild-type *C. glutamicum* ATCC 13032 (Ma et al. 2018). As a result, several mutant genes in central carbon metabolism, amino acids metabolism, cofactors and vitamins metabolism, and membrane transport systems were found relating to the efficient synthesis of BCAA. In this study, the metabolic and gene transcriptional pattern of these two BCAA producers were detected and compared with those of wild-type *C. glutamicum* ATCC 13032. The objective of this study was to explore the differences of gene transcription and intracellular metabolites between BCAA producers and the wild-type strain and to discuss how these differences can lead to changes in BCAA production.

Materials and methods

Bacterial strains and culture

The L-leucine-producing strain *Corynebacterium glutamicum* CP and the L-valine-producing strain *C. glutamicum* XV were obtained by multiple rounds of random mutagenesis and selection. These strains are accessible at the China General Microbiological Culture Collection Center with the identifiers of CGMCC 11425 (CP) and CGMCC 1.15672 (XV). The wild-type *C. glutamicum* ATCC 13032 was used as the reference strain. Bacteria were routinely cultivated at 32 °C in Luria-Bertani medium containing 1% (*w/v*) tryptone, 0.5% (*w/v*) yeast extract, and 1% (*w/v*) NaCl with 0.5% (*w/v*) glucose for 24 h. For fed batch fermentation, strains were cultivated in 5-L fermentor at 32 °C in medium containing (per liter) 80 g of glucose, 2 g of yeast extract, 3% (*v/v*) corn steep liquor, 2 g of sodium citrate, 2 g of KH_2PO_4, 1 g of $MgSO_4 \cdot 7H_2O$, 10 mg of $FeSO_4 \cdot 7H_2O$, 10 mg of $MnSO_4 \cdot H_2O$, and 10 mg of thiamine. During the fermentation process, the pH was maintained at approximately 7.0 by addition of NH_4OH (25%, *v/v*) and the concentration of glucose in the culture was maintained at or above 2% (*w/v*) by feeding with glucose (80%, *w/v*).

RNA extraction and sequencing

Cells were collected during exponential growth (at 6 h) and stationary growth (at 14 h). Total RNA was extracted (three independent repeats per condition) using the TaKaRa MiniBEST Universal RNA Extraction Kit (TaKaRa, Dalian, China) according to the manufacturer's instructions. RNA concentrations were determined by Qubit fluorometer (ThermoFisher Scientific, Waltham, USA). Sequencing libraries were generated using NEBNext® Ultra™ RNA Library Prep Kit for Illumina® (NEB, Ipswich, USA) following the manufacturer's recommendations, and index codes were added to attribute sequences to each sample. The library preparations were sequenced by Illumina HiSeq 2500 platform (Illumina, San Diego, USA) and 100 bp paired-end reads were

generated. After data filtering and quality assessment, there were more than 7 million clean reads and more than 1 Gb clean bases for each sample. The GC content of reads in each sample was in the range of 55–57%.

Differential expression analysis

After data filtering and quality assessment, reads were mapped to the XV genome. The complete genome sequence and gene annotation files are available from the GenBank database with accession number CP018175.1. The index of the reference genome was constructed using Bowtie v2.0.6 (Langmead et al. 2009) and paired-end clean reads were aligned to the reference genome using TopHat v2.0.9 (Trapnell et al. 2009).

HTSeq v0.6.1 was used to count the reads numbers mapped to each gene (Anders et al. 2015). Then, the FPKM value (expected number of fragments per kilobase of transcript sequence per millions base pairs sequenced) of each gene was calculated based on the length of the gene and the number of reads that mapped to that gene (Mortazavi et al. 2008).

Differential expression analysis was performed using the DESeq R package v1.10.1 (Anders 2010). DESeq provides statistical routines to assess differential expression in digital gene expression data using a model based on the negative binomial distribution. The resulting *P* values were adjusted using Benjamini and Hochberg's approach to control the false discovery rate (Benjamini and Hochberg 1995). Genes with an adjusted *P* value < 0.05 found by DESeq were assigned as differentially expressed.

Nucleotide sequence accession numbers

All RNA-Seq data for both conditions have been deposited in the NCBI Sequence Read Archive (SRA) under accession numbers SRP143929 (CP), SRP143974 (XV), and SRP144107 (ATCC 13032). The genome sequences of *C. glutamicum* CP and *C. glutamicum* XV are available at GenBank with accession number that chromosome of CP (CP012194.1), plasmid of CP (CP012412.2), chromosome of XV (CP018175.1), and plasmid of XV (CP018174.1).

Validation of RNA-Seq data by RT-PCR

Total RNA was reversely transcribed to cDNA using the PrimeScript RT Master Mix (TaKaRa, Dalian, China). The transcriptional levels of different genes were determined by fluorescence quantitative RT-PCR using the cDNA as the templates. The primers used in this study were listed in Supplementary Table S1. Fluorescent quantitative RT-PCR was performed using the SYBR® Premix Ex Taq™ II (Tli RNaseH Plus) (TaKaRa, Dalian, China). The parameter settings for amplification of DNA were as follows: 95 °C for 30 s, followed by 40 cycles of 95 °C for 5 s, and 60 °C for 35 s, and then, a dissociation stage of 95 °C for 15 s, 65 °C for 35 s, and 95 °C for 15 s. The transcriptional level of 16S ribosomal RNA was used as an internal reference.

Intracellular metabolites analysis

Samples for metabolic analysis were collected from the same culture and at exponential growth (at 8 h) and stationary growth (at 16 h). Cells were centrifuged (10,000×*g*, 5 min, 4 °C) and washed with 50 ml 0.9% NaCl at 4 °C. After centrifugation (10,000×*g*, 5 min, 4 °C), 50-mg wet cell pellets were resuspended in 1-ml PBS buffer (pH 8.0, 4 °C) and 20 μL deuterium-labeled succinate (1 mg/mL) was added as an internal standard. Intracellular metabolites were extracted by five freeze-thaw cycles and ultrasonication (10 min, 4 °C). Finally, the solvent mixture was centrifuged (10,000×*g*, 5 min, 4 °C) and 1 mL of the supernatant was transferred to a new 1.5-mL tube and completely dried in a Vacuum Freeze Dryer (Gold-Sim, Los Angeles, USA). The dried samples were derivatized with 40 mg/L methoxyamine in 20 ml pyridine at 30 °C for 90 min and 45 μL of N-methyl-N-(trimethylsilyl) trifluoroacetamide (MSTFA) (Sigma-Aldrich, St. Louis, USA) at 37 °C for 30 min. An Agilent 7890A-5975C GC–MS system (Agilent Technologies, Santa Clara, USA) and an HP-5 ms column (60 m × 0.32 mm, 0.25-μm film thickness) (Agilent Technologies, Santa Clara, USA) were used for metabolite analysis. The sample was injected into the GC under split mode (helium total flow rate 9 mL/min with a sweeping rate of 3 mL/min). The initial oven temperature was 70 °C for 2 min and then increased to 290 °C at 4 °C/min. Mass spectra were recorded using full scan mode. The temperatures of the injection port, ion source, transfer line, and quadrupoles were set at 250 °C, 230 °C, 280 °C, and 150 °C, respectively.

Determination of NADP(H) and NAD(H) concentrations

Cells were collected in exponential phase (at 8 h) and stationary phase (at 16 h). The intracellular NAD^+, NADH, $NADP^+$, and NADPH concentrations were measured using a coenzyme I NAD(H) assay kit and a coenzyme II NADP(H) assay kit (Jiancheng, Nanjing, China) according to the manufacturer's instructions. The protein concentrations in cleared lysates were estimated by a dye-binding method (Sedmak and Grossberg 1977), using BSA as a standard.

Results and discussion

Cell growth and titer

The L-leucine-producing strain *C. glutamicum* CP, L-valine-producing strain *C. glutamicum* XV, and wild-type *C. glutamicum* ATCC 13032 were separately cultivated in a 5-L fermentor and samples were collected at exponential growth phase and stationary growth phase and subjected to transcriptomic and metabolomics analysis. Cell growth, glucose consumption, and BCAA production were measured and are shown in Fig. 1. BCAA producers showed a lower cell density and glucose consumption than the wild-type strain. At 32 h, the cell density of XV was just 37.2% of the density of wild type and CP was 75.5% of that of wild type. XV exhibited the lowest glucose consumption (164 g/L), followed by CP (172 g/L), and wild type (228 g/L). Interestingly, XV exhibited the highest titer production and glucose-product conversion ratio. The L-valine titer of XV was 44.6 g/L with a conversion ratio of 27.2%, and the L-leucine titer of CP was 30.2 g/L with a conversion ratio of 17.6%. These results suggested that CP utilized more glucose during cell growth and replication, but XV utilized glucose more efficiently for the synthesis of L-valine.

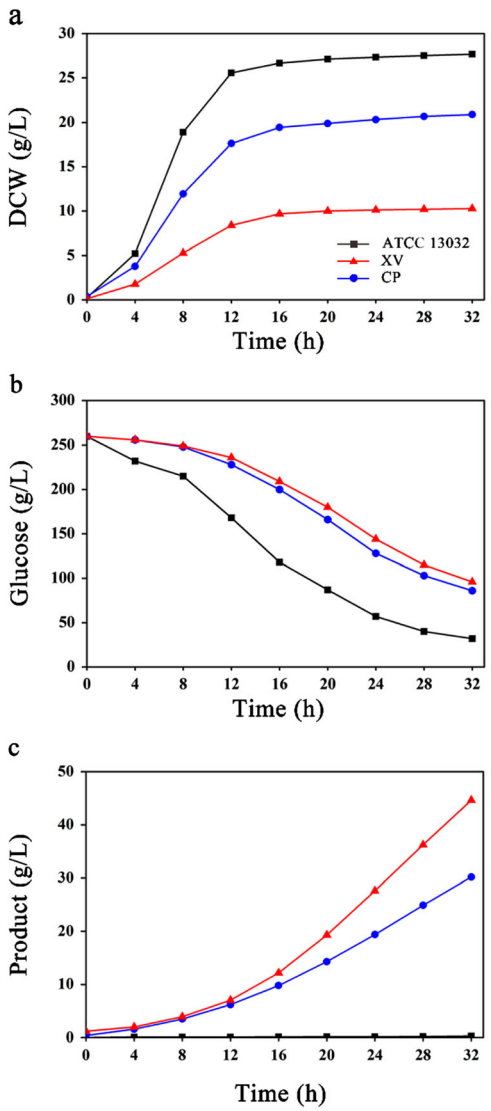

Fig. 1 Fermentation curves. (**a**) Biomass, (**b**) sugar consumption, and (**c**) product synthesis

Overview of transcriptomic and differentially expression analysis

The transcriptomes of BCAA producers and wild type in exponential phase and stationary phase were analyzed by RNA-Seq. Total RNA were extracted from different samples and mRNA was subsequently isolated to construct paired-end cDNA libraries after reverse transcription (three independent repeats per sample). Libraries were sequenced by Illumina HiSeq system, and produced greater than 7 million clean reads and greater than 1 Gb clean bases for each sample. Reads of each sample were mapped onto the XV genome. The data were normalized and presented as the FPKM, expected number of fragments per kilobase of transcript sequence per millions base pairs sequenced (Supplementary Table S2 and S3). To assess significant difference, median of fold change of each sample was used as the cutoff. All up- or downregulated genes were annotated with KO number according to the KEGG Orthology Database. Then, the functions of these genes were identified by Kyoto Encyclopedia of Genes and Genomes (KEGG) pathway analysis (Supplementary Table S4). Genes with significant differences in expression were screened using DESeq v1.10.1. The transcriptional level of these genes between the BCAA producers and the wild-type strain were visually compared by the construction of volcano plots, as presented in Figs. 2 and 3.

Overview of metabolomics analysis

GC–MS using MSTFA derivatization was used to measure the levels of intracellular metabolites in central carbon metabolism, amino acids, and non-amino organic acids. The metabolic chart shown in Fig. 4 details the amounts (μM/g cell) of intracellular metabolites detected in exponential phase (at 8 h) and stationary phase (at 16 h) samples of the different strains. As expected, a large amount of L-leucine was detected in CP and a greater amount of L-valine was detected in XV. The intracellular content of other amino acids was very low or not detected. Of the detected amino acids, the intracellular levels of L-serine, L-glutamate, and L-alanine of the BCAA producer strains were lower than those of wild type. Moreover, the intracellular pantothenate level of XV was significantly lower than in the other strains, which consistent with that XV was a pantothenate auxotroph mutant. In central

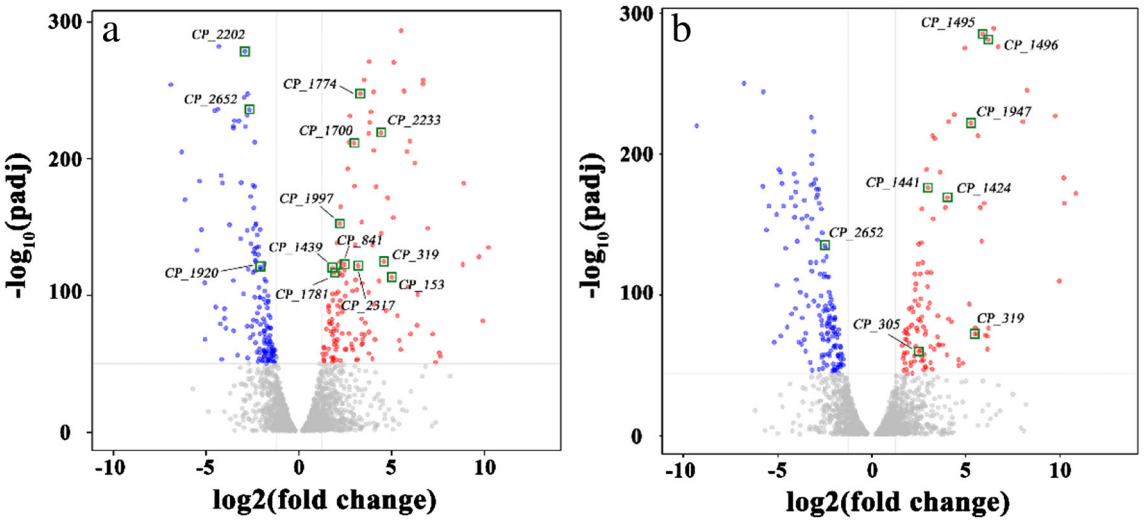

Fig. 2 Volcano plots of the differentially expressed genes (DEGs) identified between L-leucine producer *C. glutamicum* CP and wild-type *C. glutamicum* ATCC 13032. (**a**) Exponential phase, (**b**) stationary phase. In this volcano plot, the *x*-axis plots the distribution of fold change and the *y*-axis plots the logarithm of p-adj values of each identified DEG. Red dots are the genes that are upregulated in CP, blue dots are the genes that are downregulated in CP, and the dots in the green box are related to the synthesis of BCAA

carbon metabolism, BCAA producers showed a higher intracellular glucose level, but the intracellular levels of metabolites in glycolysis and even organic acids involved in the tricarboxylic acid (TCA) cycle such as citrate, isocitrate, fumarate, malate, and oxaloacetate were obviously lower in both BCAA producers than wild type.

Transcriptional and metabolic patterns of glucose uptake and glycolysis

Central metabolism glucose uptake, glycolysis, TCA cycle, and amino acid metabolism play important roles in cell growth (Reimonn et al. 2016; Huang et al. 2017). In *C. glutamicum*, carbon source uptake relies on the phosphotransferase system (PTS). Glucose is transported and simultaneously phosphorylated to glucose-6-phosphate by PTS, and an equal mole of phosphoenolpyruvate (PEP) is converted to pyruvate (Gaigalat et al. 2007). Normally, intracellular phosphorylated glucose is first metabolized by glycolysis and concomitantly generates a variety of metabolic precursors and a little energy. The L-valine producer XV had the lowest glucose consumption rate, but no mutation was identified in genes related to glucose uptake between CP and XV. However, the *pgi* and *pfkA*

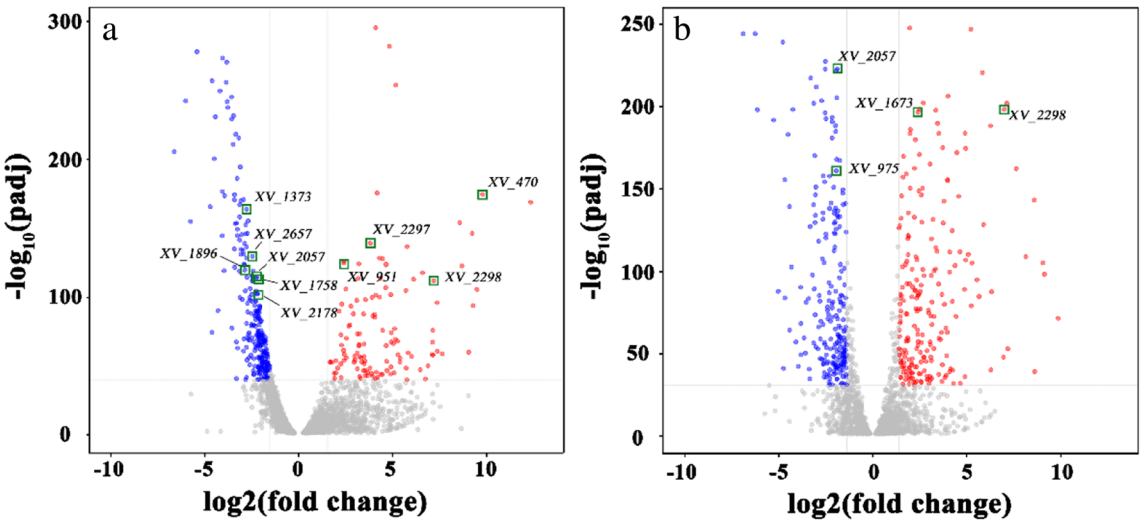

Fig. 3 Volcano plots of the differentially expressed genes (DEGs) identified between L-valine producer *C. glutamicum* XV and wild-type *C. glutamicum* ATCC 13032. (**a**) Exponential phase, (**b**) stationary phase. In this volcano plot, the *x*-axis plots the fold change and the *y*-axis plots the logarithm of p-adj values of each identified DEG. Red dots are the genes that are upregulated in XV, blue dots are the genes that are downregulated in XV, and dots in the green box are related to the synthesis of BCAA

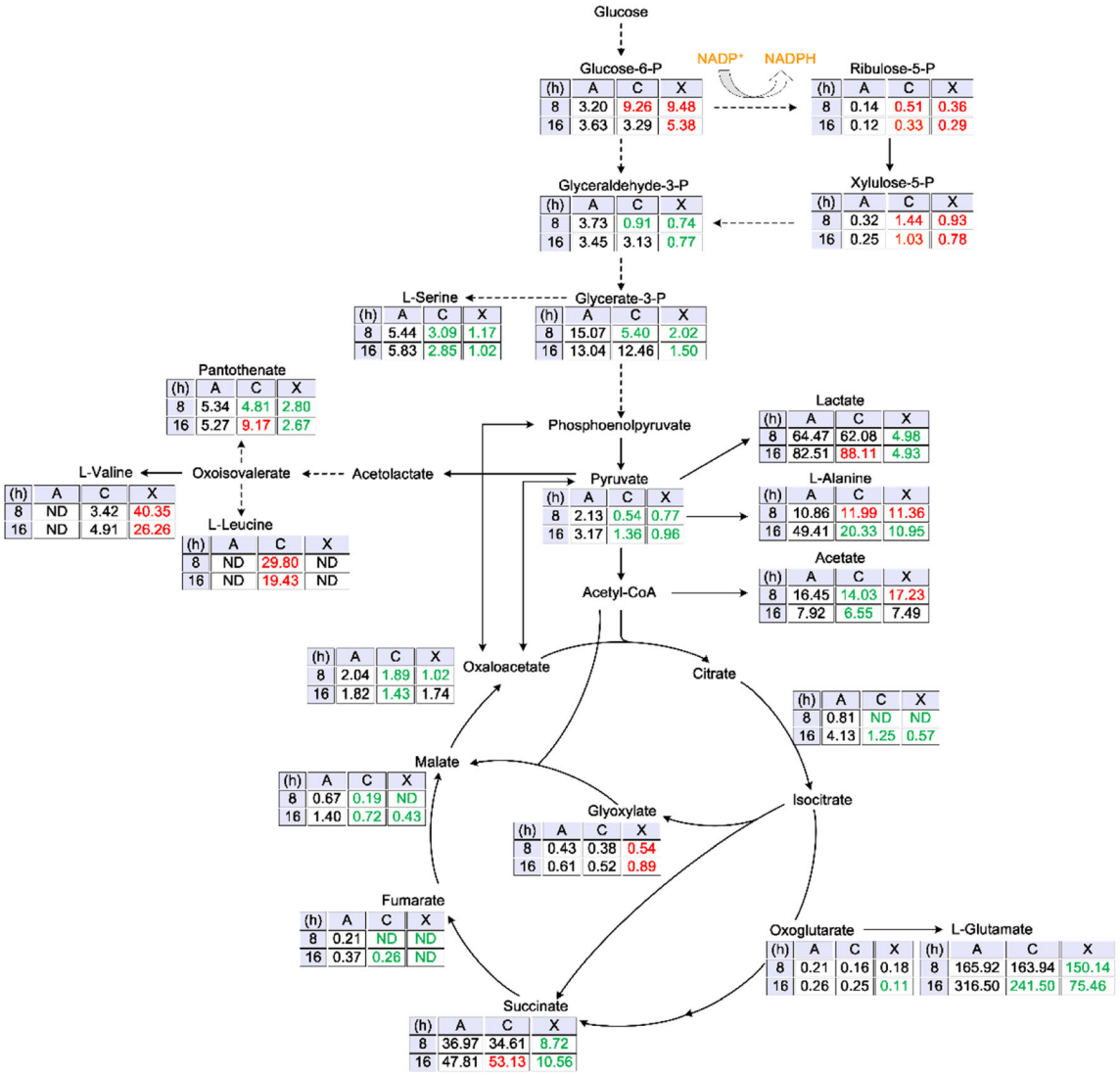

Fig. 4 Schematic overview of the metabolic pathways associated with the intracellular metabolite levels (μM/g cell) identified in BCAA producers (*C. glutamicum* CP and *C. glutamicum* XV) and wild-type *C. glutamicum* ATCC 13032. *Red numbers*, upregulated metabolites ($P < 0.05$); *green numbers*, downregulated metabolites ($P < 0.05$)

(*Cgl1250*) genes in the glycolysis pathway were mutant in the BCAA producers.

To further study the differences of glucose metabolism between the BCAA producers and the wild type, transcriptional levels of genes involved with PTS and glycolysis were investigated and visualized by heat map, as shown in Fig. 5a. There was no obvious difference between BCAA producers and wild type except for the downregulation of the glucose-transport-related gene *ptsG* in the BCAA producers. This would suggest a lower glucose uptake rate in the BCAA producers compared to the wild type. However, as shown in Fig. 4, the intracellular glucose levels in CP and XV were about 3 times higher than wild type in the exponential phase. However, the intracellular levels of glyceraldehyde-3P, glycerate-3P, and pyruvate were all significantly lower in the BCAA producers compared to wild type. These results suggested that the mutation of *pgi* and *pfkA* (*Cgl1250*) genes affected the distribution ratio of glucose between the glycolysis pathway and the pentose phosphate pathway (PPP); however, the main reason of the low glucose utilization rate of BCAA producers was probably due to other reasons than PTS and glycolysis.

Transcriptional and metabolic patterns of central carbon metabolism

Pyruvate is an important intermediate metabolite in central carbon metabolism and is completely required for BCAA synthesis (Wieschalka et al. 2012). Pyruvate was first converted into acetyl-CoA and then entered into the TCA cycle to provide a variety of organic acids and a large amount of energy for cell growth (Bott 2007). In addition, pyruvate and PEP can

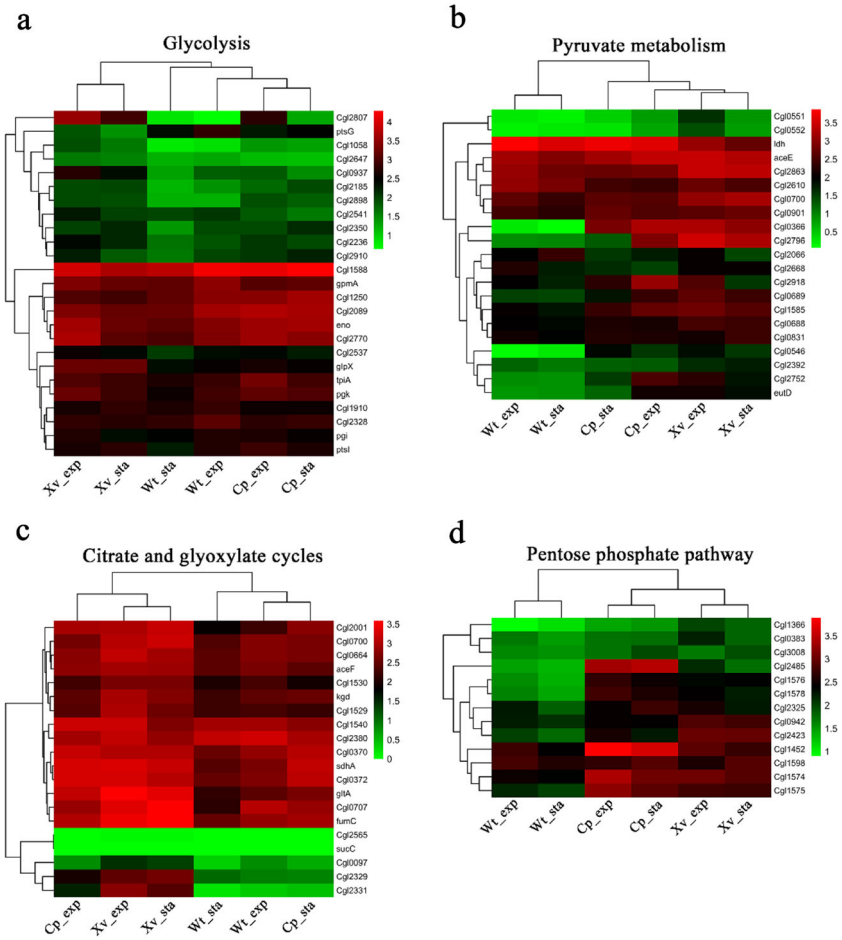

Fig. 5 Heat maps of differentially expressed genes involved in different metabolic pathways in different growth phases in the BCAA producers (*C. glutamicum* CP and *C. glutamicum* XV) and wild-type *C. glutamicum* ATCC 13032. (**a**) Glycolysis, (**b**) pyruvate metabolism, (**c**) citrate and glyoxylate cycles, and (**d**) pentose phosphate pathway. *Red* and *green* indicate higher or lower expression, respectively. "*Exp*" and "*sta*" indicate exponential phase and stationary phase, respectively

also directly enter the TCA cycle by the carboxylation reaction. Several genes involving pyruvate metabolism were mutant in the BCAA producers including coding genes of such as pyruvate kinase, PEP synthase, pyruvate carboxylase, PEP carboxylase, PEP carboxykinase and malic enzyme, and other genes involved in organic acid synthesis from pyruvate. Besides, the oxoglutarate decarboxylase coding gene *kgd* was mutant in the XV.

The transcriptional levels of genes involved in pyruvate metabolism were visualized by heat map in Fig. 5b. Genes with differentially expression were verified by using qRT-PCR (Fig. 6). The annotation features of these genes are shown in Table 1. Genes *Cgl0366* and *Cgl0688*, which involve the synthesis of acetyl-CoA, and genes *Cgl1585* and *Cgl0689*, which encode PEP carboxylase and pyruvate carboxylase, respectively, were all upregulated in BCAA producers. However, the intracellular levels of pyruvate, oxaloacetate, and other organic acids in the TCA cycle of BCAA producers were obviously lower than those of wild type. This indicated that since a great deal of pyruvate was utilized to synthesize BCAA, the supply of pyruvate available for the TCA cycle was insufficient in BCAA producers. To compensate, the upregulation of *Cgl0366* and *Cgl0688* could promote more pyruvate to form acetyl-CoA and the upregulation of *Cgl1585* and *Cgl0689* could

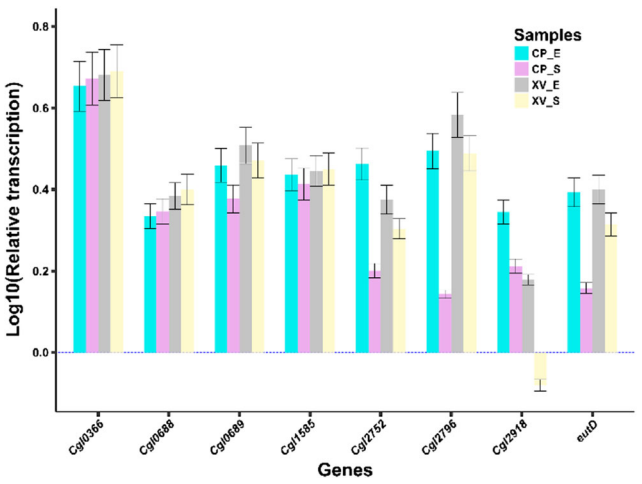

Fig. 6 Validation of the transcriptional level of pyruvate metabolism genes with differential expression by qRT-PCR. Gene transcription was normalized to the transcriptional level in the exponential phase or stationary phase of wild-type ATCC 13032. Relative transcription is presented as the log10-fold change. Data are presented as means ± standard deviation of three biological replicates. "*E*" and "*S*" indicate exponential phase and stationary phase, respectively

Table 1 Annotation feature of genes involving in the pyruvate metabolism, citrate cycle and glyoxylate cycle, pentose phosphate pathway and BCAA synthesis pathway

Gene name	Gene ID	KO	Products
Pyruvate metabolism			
Cgl0366	NCgl0355	K00382	Dihydrolipoamide dehydrogenase
Cgl0688	NCgl0658	K00382	Flavoprotein disulfide reductase
Cgl0689	NCgl0659	K01958	Pyruvate carboxylase
Cgl1585	NCgl1523	K01595	Phosphoenolpyruvate carboxylase
Cgl2752	NCgl2656	K00925	Acetate kinase
Cgl2796	NCgl2698	K00138	NAD-dependent aldehyde dehydrogenase
Cgl2918	NCgl2817	K00101	L-lactate dehydrogenase
eutD	NCgl2657	K13788	Phosphotransacetylase
Citrate cycle and glyoxylate cycle			
Cgl0097	NCgl0096	K01637	Thiamine pyrophosphate-requiring enzyme
Cgl0370	NCgl0359	K00241	Hypothetical protein
Cgl0372	NCgl0361	K00240	Succinate dehydrogenase/fumarate reductase iron-sulfur subunit
Cgl0707	NCgl0677	K01966	Detergent sensitivity rescuer dtsR2
Cgl2329	NCgl2247	K01638	Malate synthase G
Cgl2331	NCgl2248	K01637	Isocitrate lyase
fumC	NCgl0967	K01679	Fumarate hydratase
gltA	NCgl0795	K01647	Type II citrate synthase
sdhA	NCgl0360	K00239	Succinate dehydrogenase flavoprotein subunit
Pentose phosphate pathway			
Cgl1452	NCgl1396	K00033	6-phosphogluconate dehydrogenase
Cgl1574	NCgl1512	K00615	Transketolase
Cgl1575	NCgl1513	K00616	Transaldolase
Cgl1576	NCgl1514	K00036	Glucose-6-phosphate 1-dehydrogenase
Cgl1578	NCgl1516	K01057	6-phosphogluconolactonase
Cgl1598	NCgl1536	K01783	Ribulose-phosphate 3-epimerase
BCAA synthesis pathway			
brnF	NCgl0254	–	Branched-chain amino acid ABC transporter permease
brnE	NCgl0255	–	Hypothetical protein
Cgl0248	NCgl0245	K01649	2-isopropylmalate synthase
Cgl1268	NCgl1219	K01687	Dihydroxy-acid dehydratase
Cgl1271	NCgl1222	K01652	Acetolactate synthase 1 catalytic subunit
Cgl1273	NCgl1224	K00053	Ketol-acid reductoisomerase
Cgl1286	NCgl1237	K00052	3-isopropylmalate dehydrogenase
Cgl1315	NCgl1262	K01703	Isopropylmalate isomerase large subunit
Cgl2204	NCgl2123	K00826	Branched-chain amino acid aminotransferase
Cgl2844	NCgl2747	K14260	Aminotransferase
ilvH	NCgl1223	K01653	Acetolactate synthase 3 regulatory subunit
leuD	NCgl1263	K01704	Isopropylmalate isomerase small subunit
lrp	NCgl0253	–	Transcriptional regulator

enhance the carboxylation of PEP and pyruvate. Some reports declared that inactivating the pyruvate dehydrogenase complex or disrupting genes *Cgl1585* or *Cgl0689* would increase the substrate-specific product yield, but during BCAA production, glucose consumption and cell growth significantly dropped (Blombach et al. 2008; Hasegawa et al. 2013). This was primarily due to the lack of pyruvate supply in the TCA cycle.

The transcriptional levels of genes in the TCA cycle and the glyoxylate cycle were visualized by heat map as presented in Fig. 5c. Genes with differential expression were verified using qRT-PCR (Fig. 7). In XV, the intracellular level of succinate, fumarate, malate, and oxaloacetate was much lower than that in other strains. This was due to the natural incompleteness of the *kgd* gene of XV, which caused disruption of the metabolism of oxoglutarate. However, genes related to the

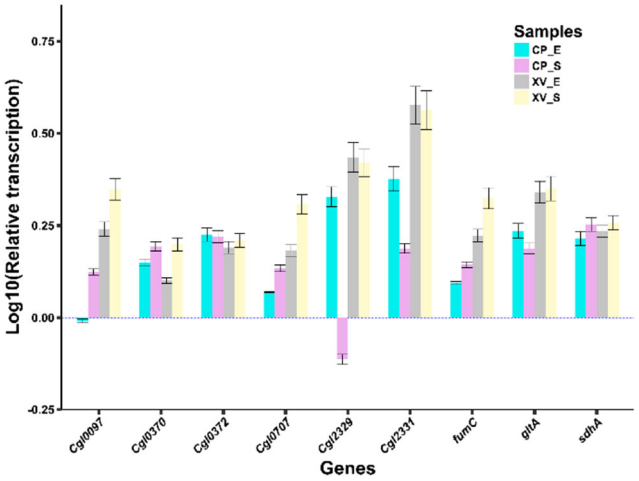

Fig. 7 Validation by qRT-PCR of the transcriptional level of genes with differential expression in the citrate and glyoxylate cycles. Transcription level was normalized to the transcriptional level in the exponential phase or stationary phase of wild-type ATCC 13032, respectively. Relative transcription is presented as the log10-fold change. Data are presented as means ± standard deviation of three biological replicates. "*E*" and "*S*" indicate exponential phase and stationary phase, respectively

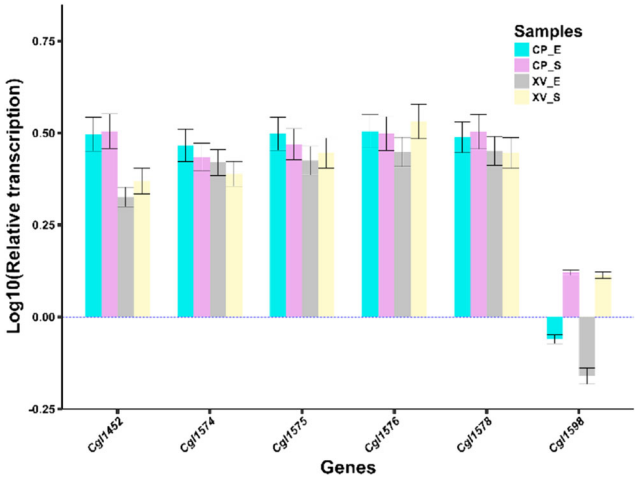

Fig. 8 Validation by qRT-PCR of the transcriptional levels of genes showing differential expression in the pentose phosphate pathway. Transcription levels were normalized to the transcriptional level in the exponential phase or stationary phase of wild-type ATCC 13032. The relative is presented as the log10-fold change. Data are presented as means ± standard deviation of three biological replicates. "*E*" and "*S*" indicate exponential phase and stationary phase, respectively

glyoxylate cycle, *Cgl2329* and *Cgl2331*, were upregulated in XV, correlating with an increase in the intracellular glyoxylate level. These results indicated that the glyoxylate cycle of XV was more active than other strains, which acted to salvage the TCA cycle deficiency. This strategy avoided the decarboxylation reaction in the TCA cycle and improved the efficiency of glucose utilization to synthesize BCAA.

Transcriptional and metabolic patterns of pentose phosphate pathway

The PPP is an alternative pathway for glucose metabolism, in which hexose is converted into pentose and generates NADPH. NADPH is an essential cofactor for cell growth and is a limiting factor for the production of various amino acids including BCAA (Bommareddy et al. 2014). The transcriptional levels of genes in PPP were visualized by heat map, as presented in Fig. 5d. Genes with differential expression were verified by using qRT-PCR (Fig. 8). In the PPP, the NADPH synthesis-related genes, *Cgl1576*, *Cgl1578* and *Cgl1452*, were mutant in the BCAA producers. While, the transcription of these three genes were both obviously upregulated in the BCAA producers. In addition, the intracellular levels of ribulose-5P and xylulose-5P were correspondingly increased (Fig. 4). Due to the requirement of a large amount of NADPH for BCAA synthesis, BCAA producers enhanced the proportion of carbon metabolic flux in the PPP to increase the NADPH supply. This also contributed to the decrease in the intracellular level of metabolites during glycolysis.

To test this hypothesis, the intracellular NAD^+, NADH, $NADP^+$, and NADPH levels of different strains were assayed (Fig. 9). Since the synthesis of BCAA would cause more NADPH consumption, the intracellular NADPH content of BCAA producers should be lower than that of wild type. However, the NADPH levels of the three strains were similar in the exponential phase and even higher in the BCAA producers than wild type in the stationary phase. Moreover, as listed in Table 2, there was no significant difference in the NADP(H)/NAD(H) ratio among strains. These characteristics are similar to that of the previously reported L-valine-producing mutant *C. glutamicum* VWB-1, which showed a faster NADPH generation rate than parent strain (Zhang et al. 2018). This results further demonstrated the increased activity of the BCAA producers' carbon metabolism in PPP.

Genes *Cgl1574*, *Cgl1575*, and *Cgl1598*, which promote the re-entering of pentose into the glycolysis pathway, were also mutant in the BCAA producers and their transcription was upregulated in BCAA producers (except *Cgl1598* downregulated in exponential growth phase). This indicated that, in BCAA producers, glucose was primarily metabolized in PPP. However, after the generation of NADPH, carbon would re-enter the glycolysis pathway to further generate pyruvate. This strategy simultaneously ensured the supply of pyruvate and the generation of NADPH.

Differences in BCAA synthesis metabolism

The key enzyme coding genes *ilvBN* and *leuA* were mutant in the BCAA producers. These mutations had been proved playing an important role in the efficient synthesis of L-leucine or L-valine. As expected, the intracellular L-leucine level of CP and L-valine level of XV were significantly higher

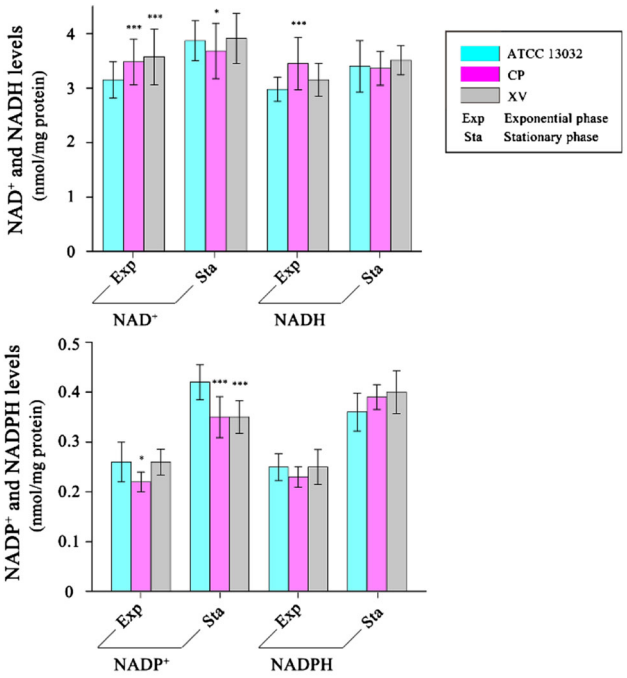

Fig. 9 Total NADP(H) and NAD(H) of BCAA producers and wild-type *C. glutamicum* ATCC 13032 in exponential phase and stationary phase during the fermentation process. Data are presented as means ± standard deviation of three independent experiments. $*P \leq 0.05$, $***P \leq 0.001$

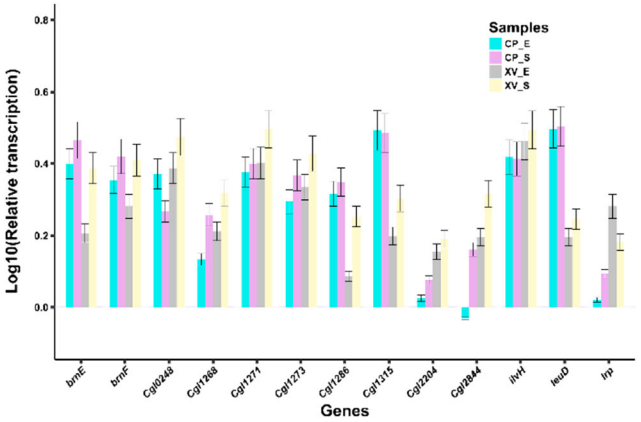

Fig. 10 Validation by qRT-PCR of the transcriptional levels of genes showing differential expression in the BCAA synthesis pathway. The levels of transcription were normalized to the transcriptional level in the exponential phase or stationary phase of wild-type ATCC 13032. The relative transcription is presented as the log10-fold change. Data are presented as means ± standard deviation of three biological replicates. "*E*" and "*S*" indicate exponential phase and stationary phase, respectively

than the other strains, and intracellular L-leucine and L-valine were not detected in the wild-type strain. This result demonstrated that the mutant key enzymes of CP and XV relieved feedback inhibition, so that product could be accumulated to a high intracellular concentration (Yin et al. 2012). Besides, since XV is a pantothenate auxotroph mutant due to the mutation of *panB* and *panC* genes, the intracellular pantothenate level was significantly lower in this strain compared to the other strains. Interestingly, 3-methyl-2-oxobutanoate is the precursor of pantothenate as well as L-valine and L-leucine, so pantothenate deficiency optimizes precursor utilization for L-valine and L-leucine synthesis (Bartek et al. 2008).

As shown in Fig. 10, the transcriptional level of most genes related to BCAA synthesis was upregulated in the BCAA producers. However, the transaminase C (EC: 2.6.1.66, 2.6.1.2) coding gene *Cgl2844* was downregulated in CP in the exponential phase but was specifically upregulated in XV. As shown in the BRENDA Enzyme Database (https://www.brenda-enzymes.org/), this transaminase catalyzes 3-methyl-2-oxobutanoate and L-glutamate to form L-valine and 2-oxoglutarate, or 3-methyl-2-oxobutanoate and L-alanine to form L-valine and pyruvate; besides, it also catalyzes the reversible reaction of L-alanine and 2-oxoglutarate to form pyruvate and L-glutamate. As a result of the upregulation of *Cgl2844*, the intracellular levels of L-glutamate and L-alanine in XV were significantly decreased, especially in stationary phase. This indicated that L-glutamate and L-alanine were rapidly consumed in XV and the amino-group was efficiently transferred to form L-valine. Contrarily, the downregulation of *Cgl2844* might be one of the main reasons why CP rarely synthesized L-valine. Therefore, these transamination reactions play an important role in L-valine synthesis in *C. glutamicum*, where L-glutamate and L-alanine work as amino donors.

Conclusion

In this study, transcriptional levels and the amounts of intracellular metabolites were measured for two industrial BCAA-

Table 2 The redox states of the strains in different growth phases during fermentation

	Exponential phase (8 h)			Stationary phase (16 h)		
	Wild type	CP	XV	Wild type	CP	XV
NAD+/NADH	1.06 ± 0.06	1.01 ± 0.04	1.13 ± 0.02	1.14 ± 0.05	1.10 ± 0.03	1.12 ± 0.03
NADP+/NADPH	1.06 ± 0.05	0.93 ± 0.02	1.02 ± 0.04	1.18 ± 0.04	0.89 ± 0.01	0.88 ± 0.02
NADP+/NAD+	0.08 ± 0.01	0.06 ± 0.01	0.07 ± 0.01	0.11 ± 0.02	0.10 ± 0.01	0.09 ± 0.02
NADPH/NADH	0.08 ± 0.01	0.07 ± 0.01	0.08 ± 0.02	0.10 ± 0.01	0.12 ± 0.02	0.11 ± 0.01

producing *C. glutamicum* by RNA-Seq and metabolomics analysis. By combining these results with previous comparative genomic analysis, the metabolic features of BCAA producers and differences from the wild type were clearly identified. For the BCAA producers, the PPP was more active than wild type, and more NADPH was generated. Carbon was prompted to re-enter into glycolysis from PPP to generate pyruvate. Since a great deal of pyruvate was utilized to synthesize BCAA, the transcriptional level of genes relating to carboxylation of PEP and pyruvate and the formation of acetyl-CoA were both upregulated. In XV, the TCA cycle was broken at the oxoglutarate node, but the glyoxylate cycle was strengthened. This avoided the decarboxylation reaction in the TCA cycle and improved the efficiency of glucose utilization. Moreover, the upregulation of *Cgl2844* provided an efficient way for amino-group transfer for L-valine synthesis, where L-glutamate and L-alanine worked as amino donors. All these common characteristics shown by BCAA producers and the unique characteristics of the L-valine producer contributed to the efficient synthesis of target product. It provided innovative and valuable reference for the subsequent construction of metabolic engineering strains.

Acknowledgments This study was supported by the National Natural Science Foundation of China (31470211 and 31770053), Natural Science Foundation of Tianjin (17JCQNJC09500), and Tianjin Municipal Science and Technology Commission (17YFZCSY01050).

Compliance with ethical standards

Conflict of interest The authors declare that they have no conflict of interest.

Ethical approval This article does not contain any studies with human participants or animals performed by any of the authors.

Informed consent Informed consent was obtained from all individual participants included in the study.

Publisher's Note Springer Nature remains neutral with regard to jurisdictional claims in published maps and institutional affiliations.

References

Anders S (2010) Analysing RNA-Seq data with the DESeq package. Mol Biol 43(4):1–17

Anders S, Pyl PT, Huber W (2015) HTSeq–a Python framework to work with high-throughput sequencing data. Bioinformatics 31(2):166–169

Bartek T, Makus P, Klein B, Lang S, Oldiges M (2008) Influence of L-isoleucine and pantothenate auxotrophy for L-valine formation in *Corynebacterium glutamicum* revisited by metabolome analyses. Bioprocess Biosyst Eng 31:217–225

Becker J, Zelder O, Häfner S, Schröder H, Wittmann C (2011) From zero to hero–design-based systems metabolic engineering of *Corynebacterium glutamicum* for L-lysine production. Metab Eng 13:159–168

Benjamini Y, Hochberg Y (1995) Controlling the false discovery rate: a practical and powerful approach to multiple hypothesis testing. J R Stat Soc B 57:289–300

Blombach B, Schreiner ME, Bartek T, Oldiges M, Eikmanns BJ (2008) *Corynebacterium glutamicum* tailored for high-yield L-valine production. Appl Microbiol Biotechnol 79:471–479

Bommareddy RR, Chen Z, Rappert S, Zeng AP (2014) A de novo NADPH generation pathway for improving lysine production of *Corynebacterium glutamicum* by rational design of the coenzyme specificity of glyceraldehyde 3-phosphate dehydrogenase. Metab Eng 25:30–37

Bott M (2007) Offering surprises: TCA cycle regulation in *Corynebacterium glutamicum*. Trends Microbiol 15(9):417–425

Chen C, Pan J, Yang X, Guo C, Ding W, Si M, Zhang Y, Shen X, Wang Y (2016) Global transcriptomic analysis of the response of *Corynebacterium glutamicum* to vanillin. PLoS One 11:e0164955

Gaigalat L, Schlüter JP, Hartmann M, Mormann S, Tauch A, Pühler A, Kalinowski J (2007) The DeoR-type transcriptional regulator SugR acts as a repressor for genes encoding the phosphoenolpyruvate: sugar phosphotransferase system (PTS) in *Corynebacterium glutamicum*. BMC Mol Biol 8:104

Hasegawa S, Suda M, Uematsu K, Natsuma Y, Hiraga K, Jojima T, Inui M, Yukawa H (2013) Engineering of *Corynebacterium glutamicum* for high-yield L-valine production under oxygen deprivation conditions. Appl Environ Microbiol 79:1250–1257

Huang Z, Lee DY, Yoon S (2017) Quantitative intracellular flux modeling and applications in biotherapeutic development and production using CHO cell cultures. Biotechnol Bioeng 114:2717–2728

Inui M, Suda M, Okino S, Nonaka H, Puskás LG, Vertès AA, Yukawa H (2007) Transcriptional profiling of *Corynebacterium glutamicum* metabolism during organic acid production under oxygen deprivation conditions. Microbiology 153:2491–2504

Krömer JO, Sorgenfrei O, Klopprogge K, Heinzle E, Wittmann C (2004) In-depth profiling of lysine-producing *Corynebacterium glutamicum* by combined analysis of the transcriptome, metabolome, and fluxome. J Bacteriol 186:1769–1784

Langmead B, Trapnell C, Pop M, Salzberg SL (2009) Ultrafast and memory-efficient alignment of short DNA sequences to the human genome. Genome Biol 10:R25

Leuchtenberger W (1996) Amino acids–technical production and use. Biotechnology: Prod Primary Metab 6:465–502 (Second Edition)

Ma Y, Chen Q, Cui Y, Du L, Shi T, Xu Q, Ma Q, Xie X, Chen N (2018) Comparative genomic and genetic functional analysis of industrial L-leucine-and L-valine-producing *Corynebacterium glutamicum* strains. J Microbiol Biotechnol 28(11):1916–1927

Mortazavi A, Williams BA, McCue K, Schaeffer L, Wold B (2008) Mapping and quantifying mammalian transcriptomes by RNA-Seq. Nat Methods 5(7):621–628

Muffler A, Bettermann S, Haushalter M, Hörlein A, Neveling U, Schramm M, Sorgenfrei O (2002) Genome-wide transcription profiling of *Corynebacterium glutamicum* after heat shock and during growth on acetate and glucose. J Biotechnol 98:255–268

Okino S, Inui M, Yukawa H (2005) Production of organic acids by *Corynebacterium glutamicum* under oxygen deprivation. Appl Microbiol Biotechnol 68:475–480

Reimonn TM, Park SY, Agarabi CD, Brorson KA, Yoon S (2016) Effect of amino acid supplementation on titer and glycosylation distribution in hybridoma cell cultures-systems biology-based interpretation using genome-scale metabolic flux balance model and multivariate data analysis. Biotechnol Prog 32:1163–1173

Sedmak JJ, Grossberg SE (1977) A rapid, sensitive, and versatile assay for protein using Coomassie brilliant blue G250. Anal Biochem 79:544–552

Solieri L, Dakal TC, Giudici P (2013) Next-generation sequencing and its potential impact on food microbial genomics. Ann Microbiol 63:21–37

Trapnell C, Pachter L, Salzberg SL (2009) TopHat: discovering splice junctions with RNA-Seq. Bioinformatics 25(9):1105–1111

Wieschalka S, Blombach B, Eikmanns BJ (2012) Engineering *Corynebacterium glutamicum* for the production of pyruvate. Appl Microbiol Biotechnol 94(2):449–459

Vogt M, Haas S, Klaffl S, Polen T, Eggeling L, Ooyen JV, Bott M (2014) Pushing product formation to its limit: metabolic engineering of *Corynebacterium glutamicum* for L-leucine overproduction. Metab Eng 22:40–52

Yang J, Yang S (2017) Comparative analysis of *Corynebacterium glutamicum* genomes: a new perspective for the industrial production of amino acids. BMC Genomics 18(1):940

Yin L, Hu X, Xu D, Ning J, Chen J, Wang X (2012) Co-expression of feedback-resistant threonine dehydratase and acetohydroxy acid synthase increase L-isoleucine production in *Corynebacterium glutamicum*. Metab Eng 14:542–550

Zhang H, Li Y, Wang C, Wang X (2018) Understanding the high l-valine production in *Corynebacterium glutamicum* VWB-1 using transcriptomics and proteomics. Sci Rep 8(1):3632